

Transient disorder in dynamically growing networks

Rui Yang,¹ Liang Huang,¹ and Ying-Cheng Lai^{1,2}

¹*Department of Electrical Engineering, Arizona State University, Tempe, Arizona 85287, USA*

²*Department of Physics, Arizona State University, Tempe, Arizona 85287, USA*

(Received 18 August 2008; revised manuscript received 11 December 2008; published 2 April 2009)

When a certain “seed” disturbance begins to spread on a large network, the number of nodes infected is a function of time. Regarding the set of infected nodes as constituting a dynamic network that evolves continuously in time, we ask: how does the order in the collective dynamics of the network vary with time? Utilizing synchronizability as a measure of the order, we find that there exists a time at which a maximum amount of disorder corresponding to a minimum degree of synchronizability can arise before the system settles into a more ordered steady state. This phenomenon of transient disorder occurs for networks of both regular and complex topologies. We present physical analyses and numerical support to establish the generality of the phenomenon.

DOI: [10.1103/PhysRevE.79.046101](https://doi.org/10.1103/PhysRevE.79.046101)

PACS number(s): 89.75.Hc, 05.45.Xt, 05.50.+q

I. INTRODUCTION

The occurrence of a temporally disordered state before a more ordered state is reached is a common phenomenon in nonlinear dynamical systems. In the case of transient chaos, for example, starting from a random initial condition a trajectory typically exhibits chaotic behavior for a finite amount of time before settling into a regular asymptotic state such as a periodic attractor [1]. Such behaviors occur in many physical, chemical, and biological systems [2]. In a large network, temporal disorder can also arise when it subjects to sudden perturbations. Take, for example, a social network. When a disturbance (e.g., a virus) first occurred, confusion can arise so that the network is more likely to be in a disordered state. However, as individuals in the network get educated about the nature, the cause, and possible consequences of the epidemic, often they can become adaptive to it. As a result, the networked system tends to enter a more ordered (or stable) state [3].

In this paper, we address the phenomenon of transient disorder in large networks. Our approach is to consider a generic type of spreading dynamics on networks, the so-called contact process [4–6], and define a dynamically evolving oscillator network or simply *dynamic network*, which encompasses all infected nodes at any given instant of time. Such a network is dynamic because, as the spreading process continues, the set of infected nodes evolves, so does the corresponding network. To characterize the order of the network in a quantitative manner, we make use of the concept of synchronizability [7–10] that is determined by the eigenvalue spectrum of the coupling matrix of the network. In particular, we regard a network as more ordered if its synchronizability is stronger. This approach thus allows us to map the phenomenon of transient disorder, as in the aforementioned example of virus spreading in a social network, into a model framework that can be analyzed quantitatively. Our analysis and numerical computations reveal that transient disorder, or weak synchronizability, is a general phenomenon in large networks, as its occurrence is independent of the network topology.

In Sec. II, we describe a generic model for spreading dynamics and the synchronization-based approach. In Sec. III,

we present results and analytic predictions with respect to dynamical evolution of the synchronizability for regular backbone networks. Two types of connecting topologies will be analyzed: lattice and ring, as they are relevant to dynamic networks generated by the spreading in different phases. In Sec. IV, we treat complex backbone networks with random and scale-free topologies. Conclusions and a brief discussion are presented in Sec. V.

II. MODEL

We consider the general contact-process model first proposed by Harris [4] and recently adopted to complex networks [5]. The process starts from a random initial seed, i.e., a randomly selected infected node. For convenience, we say that when a node is infected, it carries a “particle” that can survive for a finite amount of time. Here, we assume that the lifetime of a particle is significantly larger than the characteristic time for the whole network to get infected so that, practically, we can set the particle lifetime to be arbitrarily large. At each time step, with probability P_s every existing particle generates an “offspring” that can leave the “parent” node to infect one of its neighbors. Specifically, suppose node v_i carries a particle at time T . A node v_j from v_i ’s immediate neighbors (the set of nodes that are directly connected to v_i) is chosen randomly. If v_j is not infected (or empty), a new particle is generated at v_j . Otherwise, if v_j is already occupied by a particle, its state remains unchanged. For $P_s > 0$, eventually all nodes in the network will be infected, but the time it takes for this to occur depends on P_s : the smaller the value of P_s , the longer it takes for the entire network to be infected. Let this time be T_0 . Thus for any $T < T_0$, there is one connected subnetwork, which contains all the infected nodes and their links, and we can address the degree of order associated with the collective dynamics on the subnetwork. Here we utilize the synchronizability as a measure of the order.

The ability for a network to be synchronized is determined by the eigenvalue spectrum of the coupling matrix. It has been known that the synchronizability can be characterized by the eigenratio $R \equiv \lambda_N / \lambda_2$, where λ_N and λ_2 are the

largest and the smallest nontrivial eigenvalues [7–10]. In general, the smaller the value of R , the more probable that the network can be synchronized. Examining the two key eigenvalues for dynamic networks as induced by spreading can then lead to an assessment of the evolution of the degree of synchronizability with time. In this paper we focus on three types of network topologies: regular, random, and scale-free.

III. REGULAR NETWORKS

To gain insight, we consider a one-dimensional ring type of network, where every node is connected to m nearest neighbors, and so the average degree (the number of links a node has) is $\langle k \rangle = m$. For such a regular backbone network, a seed infection starting from a single node will initially spread to a subnetwork that has a *lattice* structure: the boundaries at both ends are open, but eventually the whole ring network will be infected so that the boundary conditions become periodic. Figure 1(a) shows the evolution of the eigenratio of the dynamic network with time for three different values of the spreading probability P_s . The size of the backbone network that supports the spreading dynamics is $N_0 = 1000$ and the average degree is $\langle k \rangle = 100$. We observe that, for all three cases, R first increases, reaches a maximum at a particular time, then decreases and approaches a constant value, indicating a transient phenomenon. A constant R value indicates that the dynamic network has reached a steady state. To facilitate analysis, we observe that the size of the infected network, denoted by N , is a nondecreasing function of time. Thus, if we plot the eigenratio as a function of the network size N , we expect to observe a local maximum for certain value of N . Since an infected network of certain size can be reached in different times for different values of P_s , examining the properties of the network with respect to its size effectively disregards any detailed information about the timing of the infection spreading. Thus, the plot of R versus N should not depend on the specific details of the spreading dynamics. Such a result is shown in Fig. 1(b), where we see that the three data sets in Fig. 1(a) have collapsed into a single universal data set in the R - N plot. The main advantage of focusing on the R - N relation is that it can be obtained analytically for different network topologies, yielding insights into the universal occurrence of transient disordered states in network dynamics.

A. Lattice topology

In the initial phase of the spreading process, approximately, a dynamic network has a lattice topology: it is open on both ends. It is thus useful to examine the spectral properties of the lattice type of regular networks. The coupling matrix \mathbf{G} is given by $G_{ij} = -1$ for $|i-j| \leq m/2$ and $i \neq j$, $G_{ij} = 0$ for $|i-j| > m/2$, and $G_{ii} = k_i$, where $k_i = m$ is the degree of node i . For such a network of size N , we find numerically that the i th component of any eigenvector \mathbf{e} of the coupling matrix has the following approximate form:

$$e_i \approx \sqrt{\frac{2}{N}} \cos\left(\frac{f\pi i}{N} + \varphi\right), \quad (1)$$

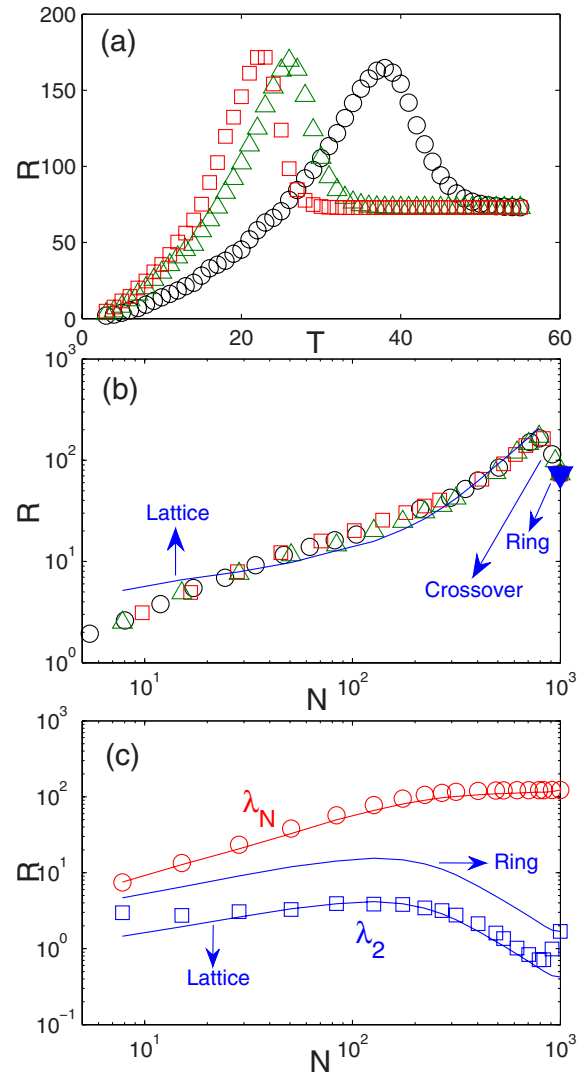


FIG. 1. (Color online) For the ring backbone network of $N_0 = 1000$ nodes and average degree $\langle k \rangle = 100$, (a) evolution of the eigenratio as a function of time for three values of the infection probability: $P_s = 0.5$ (circle), 0.8 (triangle), and 1.0 (square), (b) R versus the size of the infected network, which is apparently independent of the value of P_s , and (c) eigenvalues λ_2 and λ_N versus N . The solid curves are analytic predictions. The existence of the local maximum in R for large N can be explained theoretically by noting that a crossover from the lattice to the ring behaviors necessarily occurs for dynamic networks of large sizes (see Sec. III B). Here, all simulation results are obtained by averaging over 100 independent runs of the infection dynamics. For regular networks, since the network structure is fixed for given size and average degree, ensemble average using different network realizations is not necessary.

where $i = 1, \dots, N$, f is the basic spatial Fourier frequency ($0 \leq f < N$), and φ is the phase shift depending on the boundaries. The deviations of e_i in Eq. (1) from the actual eigenvector components occur mainly near the boundaries, i.e., for $i \sim 1$ or $i \sim N$, which can be neglected if N is large. The eigenvector is normalized: $\sum e_i^2 = 1$. By definition, the eigenvalues satisfy the eigenequation $\lambda \mathbf{e} = \mathbf{G} \cdot \mathbf{e}$ [11]. For the eigenvalue associated with the spatial frequency f , we have λ_e

$= (\mathbf{G} \cdot \mathbf{e})_i$. Expanding the right-hand side yields

$$(\mathbf{G} \cdot \mathbf{e})_i \approx \sqrt{\frac{2}{N}} \left[(m+1) \cos\left(\frac{f\pi i}{N} + \varphi\right) - \sum_{j=-m/2}^{m/2} \cos\left(\frac{f\pi(i+j)}{N} + \varphi\right) \right], \quad (2)$$

where $m/2 < i < N - m/2$. Elementary algebra gives the following result for the summation in Eq. (2),

$$\begin{aligned} \sum_{j=-m/2}^{m/2} \cos\left(\frac{f\pi(i+j)}{N} + \varphi\right) &= \frac{\sin[(m+1)f\pi/(2N)]}{\sin[f\pi/(2N)]} \cos\left(\varphi + \frac{fi\pi}{N}\right). \end{aligned}$$

We thus obtain

$$(\mathbf{G} \cdot \mathbf{e})_i \approx \left\{ m+1 - \frac{\sin[(m+1)f\pi/(2N)]}{\sin[f\pi/(2N)]} \right\} e_i, \quad (3)$$

which gives

$$\lambda \approx m+1 - \frac{\sin[(m+1)f\pi/(2N)]}{\sin[f\pi/(2N)]}. \quad (4)$$

For λ_2 and \mathbf{e}_2 , the spatial frequency is $f_2=1$. We obtain

$$\lambda_2 \approx m+1 - \frac{\sin[(m+1)\pi/(2N)]}{\sin[\pi/(2N)]}. \quad (5)$$

For λ_N , the value of the underlying spatial frequency f_N depends on network parameters. Generally, the dependence of λ on f has an attenuated wave form, and the largest value occurs at the first maximum (Fig. 2). Setting $d\lambda/df=0$ yields the following transcendental equation for determining f_N :

$$m+1 = \frac{\tan[(m+1)\pi f/(2N)]}{\tan[\pi f/(2N)]}. \quad (6)$$

Numerically, we find that this equation has multiple roots in f at the local maxima and minima of $\lambda(f)$. To obtain estimates of the roots, we note that for $m \gg 1$, the period of the function $\tan[\pi f/(2N)]$ in the denominator is much larger than that of the numerator $\tan[(m+1)\pi f/(2N)]$. Thus, in a single period of $\tan[(m+1)\pi f/(2N)]$, the denominator can be regarded as a constant. Since $m \gg 1$, Eq. (6) stipulates that the numerator be large. This can be achieved for

$$(m+1)\pi f/(2N) \approx (j+1/2)\pi,$$

where j is an arbitrary integer (Fig. 2). Note that $f=0$ is also a solution, which corresponds to the trivial minimum eigenvalue $\lambda=0$. The first peak occurs for $j=1$, i.e.,

$$(m+1)\pi f/(2N) \approx (1+1/2)\pi,$$

which gives $f=3N/(m+1) \equiv f_p$. We can use f_p as an approximation of f_N ,

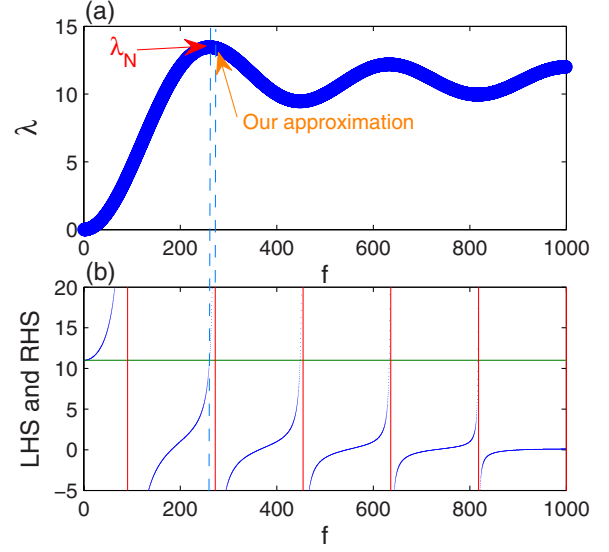


FIG. 2. (Color online) For the ring backbone network of $N_0 = 1000$ nodes and $m=10$, (a) λ versus spatial Fourier frequency f from Eq. (4), and (b) the left-hand side (LHS, horizontal line) and right-hand side (RHS, dots) of Eq. (6). The vertical lines from left to right indicate the values of f for which the equality $(m+1)\pi f/(2N) = (j+1/2)\pi$ holds for $j=0, 1, \dots, m/2$.

$$f_N \approx \frac{3N}{m+1},$$

as shown in Fig. 2(a). Moreover, since the slope of $\lambda(f)$ at λ_N is zero, a small deviation in f will lead to a much smaller variation in λ , indicating that the solution so obtained is stable. Substituting f_N back into Eq. (4), we obtain the following approximation for λ_N :

$$\lambda_N \approx m+1 + \left[\sin \frac{3\pi}{2(m+1)} \right]^{-1}. \quad (7)$$

Our derivation is based on the assumption that the eigenvectors have approximately sinusoidal forms, which neglects possible effects on the vectors from about $2m$ boundary nodes. Equations (4), (5), and (7) are thus valid for $m \ll N$ only. However, with numerical calculations we find that, although there are deviations between the predictions from Eq. (4) and the actual eigenvalues for about $2m$ eigenmodes, Eqs. (5) and (7) approximate well λ_2 and λ_N , respectively, insofar as $m < N/2$.

B. Ring topology

A ring network is a lattice with periodic boundary conditions. For such a network, we find numerically that the i th component of the normalized eigenvector \mathbf{e} can be written as

$$e_i = \sqrt{\frac{2}{N}} \sin\left(\frac{2\pi fi}{N} + \varphi\right) \quad (8)$$

for $i=1, \dots, N$, where f is an integer that satisfies $0 \leq f \leq \text{int}[(N+1)/2]$ and φ is the phase shift that can be different for different eigenvectors. Note that for the ring topology, there are no boundary effects, thus Eq. (8) is exact. Follow-

ing steps similar to those in Sec. III A, we arrive at

$$\lambda = m + 1 - \frac{\sin[(m+1)f\pi/N]}{\sin(f\pi/N)}. \quad (9)$$

Note that λ is independent of φ . Also, for $f=0$, $e_i = \sqrt{2/N}$ is independent of i , leading to $\lambda=0$. Equation (9) is accurate in the sense that varying f from 1 to $\text{int}[(N+1)/2]$ yields all the nonzero distinct eigenvalues of the coupling matrix for the ring network. In particular, λ_2 is obtained by setting $f=1$,

$$\lambda_2 = m + 1 - \frac{\sin[(m+1)\pi/N]}{\sin(\pi/N)}. \quad (10)$$

For λ_N , following the same steps of derivation as for the lattice case, we obtain $f_N \approx 3N/[2(m+1)]$ and, hence, λ_N is given by the same formula [Eq. (7)], indicating that λ_N is approximately the same for both the lattice and the ring topologies. Note that, for large N , λ_N is independent of N and it depends only on m , the average degree of the network.

Equations (9) and (10) are exact. For $N=m+1$ where m is even, we have $\sin[(m+1)f\pi/N] = \sin(f\pi) = 0$ for $f > 0$ so that Eq. (9) gives the eigenvalues of a fully (globally) connected network ($\lambda_1=0$ for $f=0$ and $\lambda_2=\dots=\lambda_N=N$ for $f > 0$). For $1 \ll m \ll N$, Eq. (7) is a good approximation for λ_N .

Figure 1(c) shows, for a ring network, the eigenvalues λ_N and λ_2 versus the size N of the spreading network. The solid curves are analytic predictions. The value of m is used as the average degree of the spreading network. We see that numerically obtained values of λ_N agree with the theoretical values very well. In particular, for N large, λ_N tends to a constant, as predicted. When N is small ($N \ll \langle k \rangle$), λ_2 is approximately given by the theoretical results of the ring network. This can be understood that, since the spreading starts from a single node and propagates to its neighbors which are interconnected with each other ($N \ll \langle k \rangle$), the resulting network forms a fully connected clique whose λ_2 is given by Eq. (10). As N approaches to and exceeds $\langle k \rangle$, the two fronts of the spreading can no longer be directly connected, thus the infected network has a lattice form with open boundaries, as shown schematically in Fig. 3(a). Indeed, numerical results agree well with the theoretical results of λ_2 for lattice networks. When the size N of the spreading network approaches the original network size N_0 , the two fronts of the spreading network meet and a ring structure is formed again, as shown schematically in Fig. 3(b). In this case, the eigenvalue λ_2 is again determined by the formula for the ring network [Eq. (10)]. We thus expect to observe a crossover of the numerical data from the lattice to the ring formula for N close to N_0 , as shown in Fig. 3(c).

IV. COMPLEX NETWORKS

A. Random networks

A random network can be generated by connecting every pair of nodes with probability p . The backbone-network size is N_0 , and the average degree of the subnetwork of size N is $\langle k \rangle = pN$. To calculate the relevant eigenvalues analytically, we note that, for the adjacency matrix \mathbf{A} , where $A_{ij} = -1$ if nodes i and j are connected and $A_{ij} = 0$ otherwise, the distri-

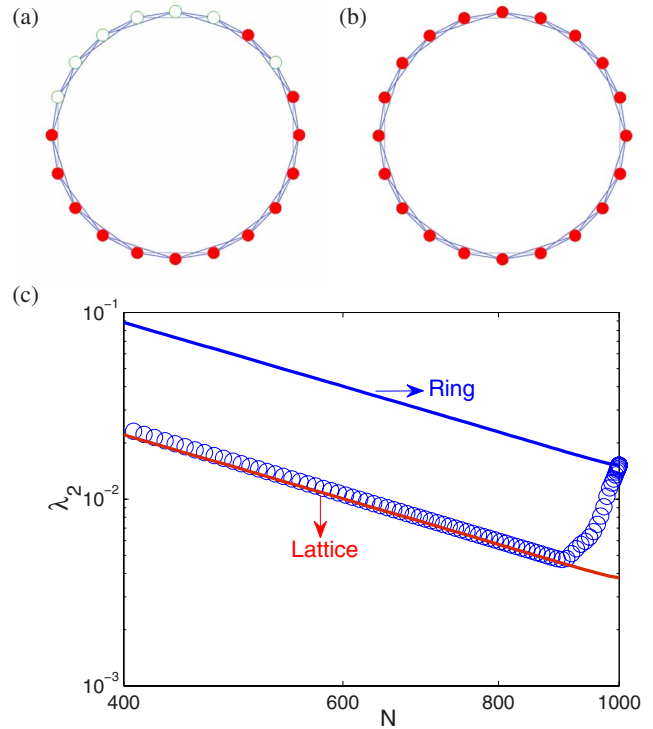


FIG. 3. (Color online) For a regular backbone network with a ring topology, (a) schematic illustration of a dynamic network in the transient phase where the infected nodes (solid circle) constitute an open latticelike network, (b) illustration of a large infected network with a ring-type topology in the steady-state phase, and (c) crossover of numerically obtained values (circles) of λ_2 from prediction based on the latticelike topology to that with the ring topology on network of $N_0=1000$ and $\langle k \rangle=100$.

bution of the eigenvalues $\lambda_i^{(A)}$ follows the Wigner semicircle law [12], where the center of the semicircle is at zero. In particular, we have

$$\lambda_1^{(A)} \approx -Np,$$

$$\lambda_2^{(A)} \approx -2\sqrt{Np(1-p)},$$

$$\lambda_N^{(A)} \approx 2\sqrt{Np(1-p)},$$

where $\sum_i \lambda_i^{(A)} = 0$. For the coupling matrix \mathbf{G} , where $G_{ij} = A_{ij}$ for $i \neq j$ and $G_{ii} = k_i$, we have $\lambda_1 = 0$ and $\text{Tr}(\mathbf{G}) = \sum_i k_i = N^2 p$. The nontrivial eigenvalues are still distributed according to the semicircle law except that the center of the semicircle is now at Np . We thus have

$$\lambda_2 \approx Np - 2\sqrt{Np(1-p)}. \quad (11)$$

The requirement that $\lambda_2 > 0$ yields, $N > N_2 = 4(1-p)/p$ for fixed value of p . Since we assume that the backbone random network is sparse, any dynamic network generated by the spreading process is also sparse. Furthermore, the initial dynamic network can be so sparse that it can be regarded as an overstretched network, i.e., a random network constructed with the same parameters N and a deduced value of p is usually not connected, which leads to a negative λ_2 in Eq.

(11). If a few (typically one or two) edges with the largest number of shortest paths passing through them are removed [13], the network will be disintegrated into two groups. Thus conceptually, such an overstretched network can be regarded as consisting of two subnetworks (or two clusters), where the numbers of nodes contained in the clusters are approximately equal and the clusters are connected by very few edges so that the probability of “intercluster” connection is small: $p_l \geq 0$. An advantage of conceptualizing such a clusteredlike structure is to make use of the theory developed in the context of synchronization in complex clustered networks [14], from which we obtain $\lambda_2 = Np_l$. Say the two clusters are connected by C links, where $C \leq 2$ is a constant. We then have $(N/2)^2 p_l = C$, i.e., $p_l \sim 1/N^2$, which gives $\lambda_2 \sim N^{-1}$. The critical value of N below which this relation holds is $N_1 = \sqrt{8/p}$, obtained by setting $C=2$. The range in the size N , $N_1 < N < N_2$, in fact defines the transition regime in which the dynamic network changes from being clustered to being random. These considerations lead to

$$\lambda_2 \sim \begin{cases} N^{-1}, & N \leq N_1 = \sqrt{8/p} \\ \text{transition,} & N_1 < N \leq N_2 = 4(1-p)/p \\ Np - 2\sqrt{Np(1-p)}, & N > N_2. \end{cases} \quad (12)$$

We now consider the largest eigenvalue λ_N . A recent result gives that for a sparse random network, $\lambda_N \approx k_{\max} + 1$ [15], where k_{\max} represents the largest degree of the infected subnetwork. For a random network, the variance σ^2 of the degree variable is $Np(1-p)$. The degree distribution $P(k)$ can be approximated by a normal distribution, $P(k) = (\sqrt{2\pi\sigma^2})^{-1} \exp[-(k-\langle k \rangle)/(2\sigma^2)]$. For a finite network, the average number of nodes that have degrees larger than k_{\max} is given by $N \int_{k_{\max}}^{\infty} P(k) dk$. If this number is less than 1, k_{\max} is the largest degree. The reasoning leads to

$$N \int_{k_{\max}}^{\infty} P(k) dk = 1. \quad (13)$$

We then have

$$N \left[\frac{1}{2} - \text{erf} \left(\frac{k_{\max} - \langle k \rangle}{[\sqrt{Np(1-p)}]^{1/2}} \right) \right] = 1, \quad (14)$$

where the error function is $\text{erf}(x) \equiv \int_0^x (2\pi)^{-1/2} e^{-y^2/2} dy$. The value of k_{\max} is thus given by

$$k_{\max} = \text{erf}^{-1} \left(\frac{N-2}{2N} \right) \sqrt{Np(1-p)} + \langle k \rangle. \quad (15)$$

Figure 4(a) shows examples of the evolution of the eigenratio with time for three values of the spreading probability P_s , where a transient disorder is observed. Changing the time variable into the size N of the dynamic network, we see that cases with different values of P_s all collapse into a single curve, as shown in Fig. 4(b). Figure 4(c) shows λ_N and λ_2 versus N , together with our theoretical predictions for λ_2 . We observe that the numerical results for λ_N (open circles) are matched very well by the quantity $k_{\max} + 1$ (open triangles),

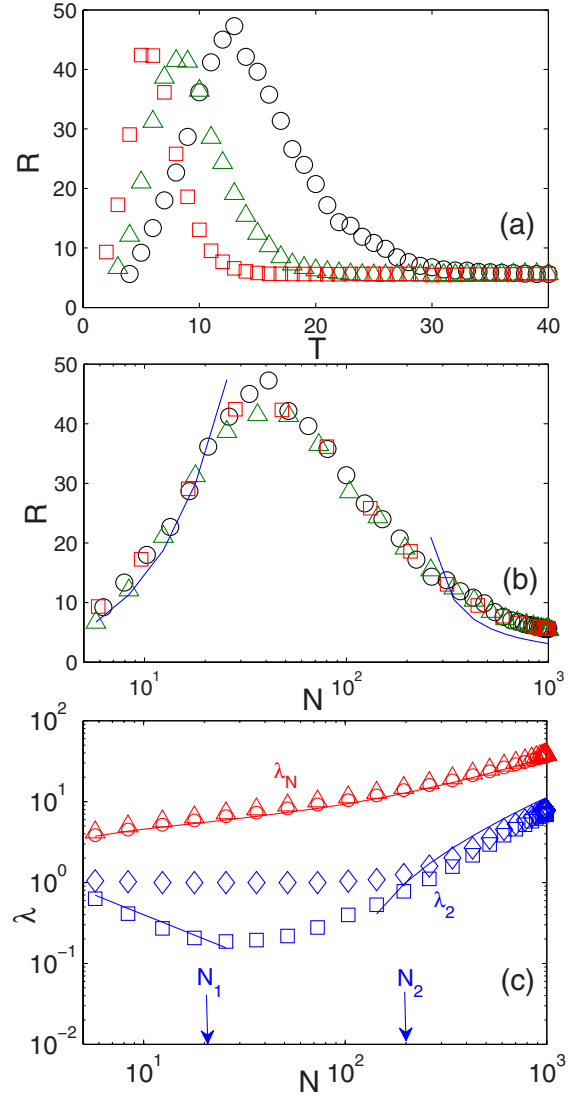


FIG. 4. (Color online) For an ensemble of random networks of fixed average degree $\langle k \rangle = 20$ and $N_0 = 1000$ nodes, (a) evolution of the eigenratio R in time for three values of the spreading probability: $P_s = 0.3$ (circle), 0.5 (triangle), and 0.8 (square), (b) R , and (c) numerical eigenvalues λ_2 and λ_N (symbols) versus the size of the dynamic network and theoretical predictions (curves). Circles: numerically obtained λ_N ; triangles: $k_{\max} + 1$; squares: numerically obtained λ_2 ; and diamonds: minimum degree. The results are obtained by averaging over 300 network realizations.

and for the regions $N < N_1$ and $N > N_2$, numerical results for λ_2 (open squares) agree with the predicted formula (solid curves) reasonably well. Our theory, however, does not predict the values of λ_2 in the transition region $N_1 < N < N_2$.

B. Scale-free networks

For a scale-free network, the degree distribution follows a power law [16]: $P(k) = ak^{-\gamma}$ for $k \geq m_0$, where $\gamma > 0$ is the degree exponent, a is a constant, and m_0 is the minimum degree of the backbone network of size N_0 . The constant a

can be determined by probability normalization: $\int_{m_0}^{\infty} P(k)dk = 1$.

To estimate the eigenvalue λ_2 , we note that because of the sparsity of the dynamic network at the beginning of the spreading process, the analysis is similar to that with random networks. We have $\lambda_2 \sim N^{-1}$ for $N \leq N_1 = \sqrt{8/p}$. When N is larger than the critical point for percolation [17], as given by

$$N_2 = N_0 \langle k \rangle / (\langle k^2 \rangle - \langle k \rangle), \quad (16)$$

the network becomes relatively less sparse and we found numerically that λ_2 can be approximated by the minimum degree m . Since the dynamic network is constructed randomly from the original network, m can be approximated by $m_0 N / N_0$ because, in general, a node has only N / N_0 fraction of its original neighbors in the dynamic network. We thus have

$$\lambda_2 \sim \begin{cases} N^{-1}, & N \leq N_1 = \sqrt{8/p} \\ \text{transition}, & N_1 < N \leq N_2 = N_0 \langle k \rangle / (\langle k^2 \rangle - \langle k \rangle) \\ m_0 \frac{N}{N_0}, & N > N_2. \end{cases} \quad (17)$$

The largest eigenvalue λ_N can be approximated by $k_{\max} + 1$ [15]. Similar to Eq. (15), k_{\max} is given by

$$k_{\max} \approx \langle k \rangle N^{1/(\gamma-1)}. \quad (18)$$

Results from Eq. (18) agree with the simulation results when the degree distribution is algebraic.

Numerical evidence for the appearance of transient disorder is shown in Fig. 5(a). Collapse of temporal evolutions of the eigenratio R for different values of the spreading probability into a single curve in the R - N plot is shown in Fig. 5(b). Support for theoretical estimates of λ_2 and λ_N is presented in Fig. 5(c). As shown in Figs. 5(b) and 5(c), when N is small, e.g., $N < 400$, the algebraic characteristic of the degree distribution is not so pronounced. In this case, there are deviations between the theoretical predictions for λ_N and R and the numerics.

V. CONCLUSIONS

In a dynamic environment where a large networked system is subject to sudden perturbations, disorder can arise. Often a disordered state lasts for a finite amount of time before the system reaches a new steady state. Examples of the appearance of such a transient disordered state abound in different contexts including nonlinear dynamical systems that model a vast variety of physical, chemical, and engineering phenomena and biological and social networks. While transient chaos in dynamical systems has been studied extensively [2], the phenomenon of transient disorder in large networked systems presents new challenges as a typical situation for such a disordered state to arise is where the backbone-network structure supporting the state is dynamic and evolves continuously in time. This is equivalent to the situation where the phase-space dimension of a dynamical system keeps increasing with time.

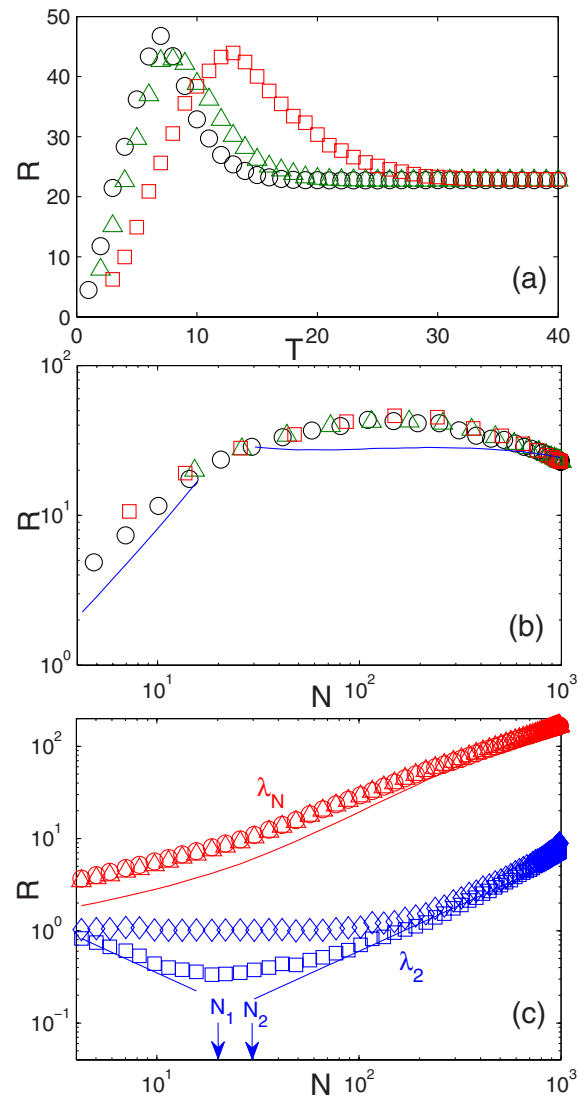


FIG. 5. (Color online) For scale-free networks of fixed average degree $\langle k \rangle = 20$ and $N_0 = 1000$ nodes, (a) evolution of the eigenratio R in time for three values of the spreading probability: $P_s = 0.5$ (square), 0.8 (triangle), and 1 (circle), [(b) and (c)] R , λ_2 , and λ_N versus the size of the dynamic network and theoretical predictions (curves). Circles: numerically obtained λ_N ; triangles: $k_{\max} + 1$; squares: numerically obtained λ_2 ; and diamonds: minimum degree. The results are obtained by averaging over 300 network realizations.

The contribution of this paper is a model paradigm that allows the transient-disorder phenomenon to be addressed systematically for large networks. There are two ingredients in our model: spreading dynamics and network synchronizability. The former determines a set of dynamically evolving subnetworks on which disorder can arise and the latter represents a convenient way to characterize the degree of disorder. Our model captures the essential features of the rise of transient disorder, or weak synchronizability, in large networks. We have provided physical analyses and numerical computations to establish the universality of the phenomenon

in both regular and complex networks. While our focus in this paper is on the dynamics of growing infected networks, a systematic investigation of how disorders or the complexity of the topology [18] changes as the infected network grows would be interesting and may deserve further efforts.

ACKNOWLEDGMENTS

We thank Yan Wang and Xiaojuan Ma for very useful discussions. This work was supported by USAFOSR under Grant No. FA9550-07-1-0045.

-
- [1] C. Grebogi, E. Ott, and J. A. Yorke, *Phys. Rev. Lett.* **48**, 1507 (1982); *Physica D* **7**, 181 (1983).
- [2] T. Tél and Y.-C. Lai, *Phys. Rep.* **460**, 245 (2008).
- [3] Examples of spreading dynamics and the rise of disorder in social networks include the transmission of severe acute respiratory syndrome (SARS) in small-world networks [N. Masuda, N. Konno, and K. Aihara, *Phys. Rev. E* **69**, 031917 (2004)] and dynamics of rumor spreading on complex networks [Y. Moreno, M. Nekovee, and A.-F. Pacheco, *ibid.* **69**, 066130 (2004)].
- [4] T. E. Harris, *Ann. Probab.* **2**, 969 (1974).
- [5] C. Castellano and R. Pastor-Satorras, *Phys. Rev. Lett.* **96**, 038701 (2006); **98**, 029802 (2007); **100**, 148701 (2008).
- [6] R. Yang, L. Huang, and Y.-C. Lai, *Phys. Rev. E* **78**, 026111 (2008).
- [7] X. F. Wang and G. Chen, *Int. J. Bifurcation Chaos Appl. Sci. Eng.* **12**, 187 (2002); *IEEE Trans. Circuits Syst., I: Fundam. Theory Appl.* **49**, 54 (2002).
- [8] M. B. Barahona and L. M. Pecora, *Phys. Rev. Lett.* **89**, 054101 (2002).
- [9] T. Nishikawa, A. E. Motter, Y.-C. Lai, and F. C. Hoppensteadt, *Phys. Rev. Lett.* **91**, 014101 (2003).
- [10] See, for example, A. E. Motter, C. Zhou, and J. Kurths, *Europhys. Lett.* **69**, 334 (2005); *Phys. Rev. E* **71**, 016116 (2005); C. Zhou, A. E. Motter, and J. Kurths, *Phys. Rev. Lett.* **96**, 034101 (2006); F. M. Atay, T. Birykoğlu, and J. Jost, *IEEE Trans. Circuits Syst., I: Regul. Pap.* **53**, 92 (2006); L. Huang, Y.-C. Lai, and R. A. Gatenby, *Chaos* **18**, 013101 (2008).
- [11] Generally the eigenvalues and the eigenvectors could be obtained simultaneously by solving the eigenequation. However, if the eigenvector has some known properties, such as possessing an approximate sinusoidal wave form, these properties can be used to significantly simplify the solutions.
- [12] E. P. Wigner, *Ann. Math.* **53**, 36 (1951).
- [13] M. E. J. Newman and M. Girvan, *Phys. Rev. E* **69**, 026113 (2004).
- [14] L. Huang, K. Park, Y.-C. Lai, L. Yang, and K. Yang, *Phys. Rev. Lett.* **97**, 164101 (2006).
- [15] D.-H. Kim and A. E. Motter, *Phys. Rev. Lett.* **98**, 248701 (2007).
- [16] A.-L. Barabási and R. Albert, *Science* **286**, 509 (1999).
- [17] D. S. Callaway, M. E. J. Newman, S. H. Strogatz, and D. J. Watts, *Phys. Rev. Lett.* **85**, 5468 (2000).
- [18] J. Kim and T. Wilhelm, *Physica A* **387**, 2637 (2008).